



Research paper

Design, synthesis and anticancer properties of novel oxa/azaspiro[4,5]trienones as potent apoptosis inducers through mitochondrial disruption



D. Yugandhar^{a, b}, V. Lakshma Nayak^a, Sivakumar Archana^a, Kunta Chandra Shekar^a,
Ajay Kumar Srivastava^{a, b, *}

^a Medicinal Chemistry and Pharmacology Division, CSIR-Indian Institute of Chemical Technology, Hyderabad, 500 007, India

^b Academy of Scientific and Innovative Research (AcSIR), NewDelhi, 110 025, India

ARTICLE INFO

Article history:

Received 25 March 2015

Received in revised form

23 June 2015

Accepted 27 June 2015

Available online 2 July 2015

Keywords:

Ipsocyclization

Oxaspiro[4,5]trienone

Azaspiro[4,5]trienone

Anticancer activity

Cell cycle analysis

Mitochondrial membrane potential ($\Delta\Psi_m$)

Western blot analysis

Apoptosis

ABSTRACT

A series of twenty seven oxa/azaspiro[4,5]trienone derivatives were synthesized and their anticancer properties have been explored. GI_{50} values of all these compounds were evaluated against four types of human cancer cell lines, i.e. MCF-7 (breast), DU-145 (prostate), A549 (lung) and HepG2 (liver). Five compounds of the series exhibited good anticancer potential against MCF-7 with GI_{50} values less than $2 \mu\text{M}$. Detailed biological studies of the two representative compounds **9b** and **9e** revealed that they arrest cell cycle in G0/G1 phase and induce mitochondria mediated apoptosis, that was further confirmed by measurement of mitochondrial membrane potential ($\Delta\Psi_m$), intracellular ROS generation, caspase 9 activity and Annexin V-FITC assay. Furthermore, western blot analysis suggested that these compounds up-regulate the levels of p53, p21, p27 and Bax, and down-regulate the level of Bcl-2 confirming the apoptosis inducing properties.

© 2015 Elsevier Masson SAS. All rights reserved.

1. Introduction

Identification of novel scaffolds with improved pharmaceutical properties is always exciting to medicinal chemists towards the development of new chemical entities (NCEs). There are several scaffolds of significant synthetic interests whose pharmaceutical properties need to be explored [1]. The newly designed molecules, mimicking drug skeletons with additional functionalities, can display improved or reduced pharmaceutical potential depending on their interactions with biological system. Hence, a detailed mechanistic investigation and structure activity relationship (SAR) studies of the new skeletons are required for developing pharmacophores with improved efficacy [2]. With the exceeding cases of cancer patients every year and lesser success in anticancer drug development, new scaffolds need to be identified as potential leads

[3]. In our efforts to study the pharmaceutical potential of new scaffolds, we have identified novel oxaspiro[4,5]trienones; **II** possessing anti-proliferative properties [4]. These spiro[4,5]trienones were designed as constrained tamoxifen; **I** mimic to develop new selective estrogen receptor modulators (SERMs), however *in vitro* screening of these compounds revealed that they are not selective towards ER positive breast cancer cell line (MCF-7) and were found to be equally potent against ER negative breast cancer cell line (MDA-MB-231) [Fig. 1] [4]. In continuation to our previous work, herein we report the detailed biological profiling of oxaspiro[4,5]trienones; **II** and azaspiro[4,5]trienones; **III** along with their structure activity relationship (SAR) studies. The literature survey shows that structurally related antitumor compounds bearing enone moiety may facilitate ROS production which in turn can induce apoptosis [Fig. 1] [5–8]. Anthracenyl amino acid **IV** [5], Dehydroaltenusin **V** [6]; a natural product isolated from a fungus *Alternaria tenuis*, and its tautomer **VI**, inhibit DNA polymerase α and induce apoptosis. Increase in ROS production by small molecules triggers the cancer cell death [7], for example, a dienone containing natural product derivative Deoxyxyloquinone **VII**

* Corresponding author. Medicinal Chemistry and Pharmacology Division, CSIR-Indian Institute of Chemical Technology, Hyderabad, 500 007, India.

E-mail address: aksrivastava@iict.res.in (A.K. Srivastava).

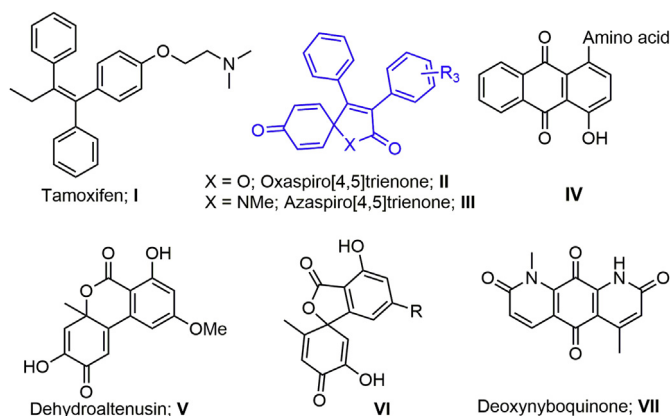


Fig. 1. Recently reported apoptosis inducing agents and our designed prototypes.

exhibits excellent tumorigenic potential in animal models through ROS generation [8].

ROS production in cancer cells regulates cellular growth, cell signaling and synthesis of important substances. Furthermore, mitochondria plays an important role for the survival of cancer cells, hence disrupting mitochondrial function by small molecules induces apoptosis [9,10]. Considering these findings from literature, we became interested to examine the apoptosis inducing properties of oxa/azaspiro[4,5]trienones.

2. Results and discussion

2.1. Chemistry

As reported in our previous communication, oxaspiro[4,5]trienones **9a-g** were obtained by coupling of compound **6** with various boronic acids; **8** under Suzuki conditions [4]. Compound **9h** was prepared by Heck reaction of **6** with methylacrylate. Azaspiro[4,5]trienones **10a-o** were synthesized from *N*-methyl-*p*-anisidine; **2** by following similar synthetic strategy. *N*-methyl-*p*-anisidine; **2** was coupled with 3-phenylpropionic acid; **3** to yield amide; **5** which was subjected to iodine mediated *ipso*-iodocyclization for the construction of compound **7**. Suzuki coupling of **7** with various

boronic acids; **8** produced **10a-o** in good yields [Scheme 1]. All the compounds were characterized by ^1H , ^{13}C NMR and HRMS analysis. Purity of all the newly synthesized compounds was checked by HPLC.

2.2. Biology

2.2.1. Anticancer activity

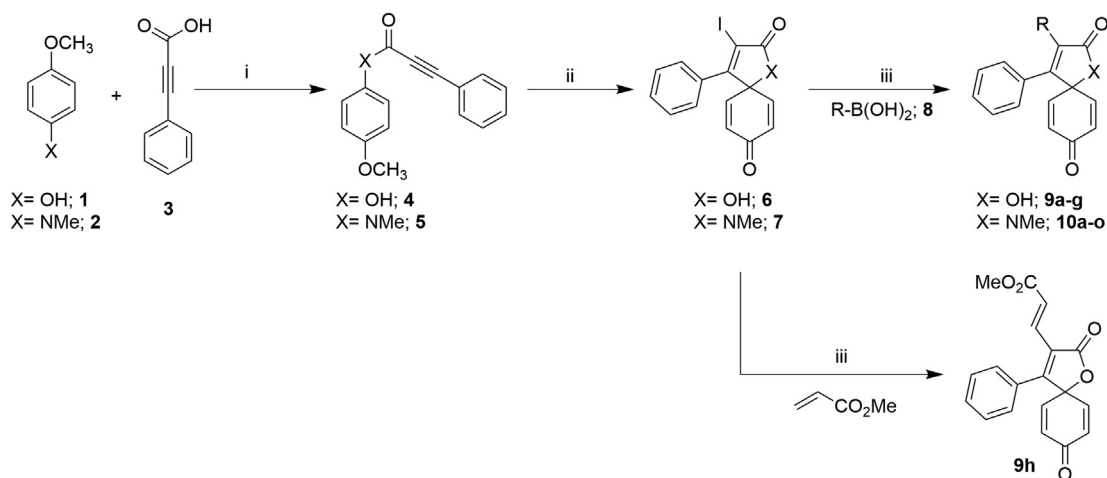
In vitro cytotoxicity of compounds **9a-h** and **10a-o** were evaluated against four types of human cancer cell lines; MCF-7 (Breast-ER positive), DU-145 (Prostate), A549 (Lung) and HepG2 (Liver) by using sulforhodamine B (SRB) method [11]. There are several rapid colorimetric assays described for *in vitro* chemo sensitivity testing of tumor cell lines. While tetrazolium [MTT; 3-(4,5-dimethylthiazolyl)-2,5-diphenyltetrazoliumbromide] assay being the most widely used, recently the US National Cancer Institute (NCI) recommended use of the sulforhodamine B (SRB) protein stain for *in vitro* chemo sensitivity testing. The SRB assay appeared to be more sensitive than MTT assay, with better linearity with cell number and higher reproducibility [12]. The compounds exhibiting $\text{GI}_{50} \leq 10 \mu\text{M}$ were considered to be active against the respective cancer cell lines. The growth inhibition data (expressed as GI_{50}) of compounds **9a-h** and **10a-o** are shown in Table 1. The results of the cytotoxicity assay showed that compounds **9b** and **9e** possess significant anti-proliferative properties against the human breast cancer cell line MCF-7. The promising activity of **9b** and **9e** prompted us to examine their pharmacological properties in detail.

2.2.2. Cell cycle analysis

In general, anticancer agents prevent cell division at various checkpoints of cell cycle, thereby decreasing the growth and proliferation of cancerous cells [13]. Cell cycle analysis after treatment with potent anticancer agents shows the distinguish cells in different phases of the cell cycle. In this study, MCF-7 cells were treated with compound, **9b** and **9e** at 0.5 and 1 μM concentrations for 48 h. The data obtained clearly indicated that these compounds (**9b** and **9e**) showed G0/G1 cell cycle arrest when compared to untreated control (Fig. 2, Table 2).

2.2.3. Measurement of mitochondrial membrane potential ($\Delta\Psi_m$)

The maintenance of mitochondrial membrane potential ($\Delta\Psi_m$) is important for mitochondrial integrity and bioenergetic function



Reagents and Conditions: i) DIC, HOBt, DCM; ii) I₂, NaHCO₃, CH₃CN; iii) Pd(OAc)₂, K₂CO₃, DMF, 80 °C

Scheme 1. Synthesis of spirotrienediones.

Table 1
Anticancer activity data of compounds **9a-h** and **10a-o**.

Entry	Compound	R	GI ₅₀ (μM)			
			MCF-7	DU-145	A549	HepG2
1	9a	4-OH-Ph	3.4 ± 0.17	2.7 ± 0.05	6.2 ± 0.03	3.5 ± 0.15
2	9b	4-NO ₂ -Ph	1.0 ± 0.04	1.9 ± 0.32	4.0 ± 0.01	1.5 ± 0.04
3	9c	4-OMe-Ph	1.8 ± 0.02	4.1 ± 0.10	7.3 ± 0.16	3.4 ± 0.23
4	9d	4-CH ₂ OH-Ph	1.7 ± 0.15	2.4 ± 0.14	8.1 ± 0.04	3.3 ± 0.15
5	9e	2-OMe,5-F-Ph	1.0 ± 0.02	0.9 ± 0.15	4.6 ± 0.14	1.4 ± 0.12
7	9f	4-CO ₂ H-Ph	3.5 ± 0.13	4.8 ± 0.04	6.3 ± 0.02	6.3 ± 0.21
8	9g	5-CHO-Thiophenyl	3.4 ± 0.01	4.0 ± 0.05	4.6 ± 0.38	2.6 ± 0.02
9	9h	–CH=CH–CO ₂ Me	1.2 ± 0.25	4.3 ± 0.37	7.8 ± 0.04	6.3 ± 0.18
10	10a	4-CH ₂ OH-Ph	7.6 ± 0.09	11.5 ± 0.56	13.6 ± 0.47	7.7 ± 0.54
13	10b	2-benzothiophenyl	4.2 ± 0.16	9.0 ± 0.31	18.8 ± 1.87	7.2 ± 0.10
14	10c	4-CF ₃ Ph	8.1 ± 0.07	17.6 ± 0.36	30.3 ± 2.83	13.7 ± 0.16
15	10d	1-Naphthyl	2.4 ± 0.08	6.3 ± 0.20	17.3 ± 0.90	6.12 ± 0.23
16	10e	Ph	8.2 ± 0.04	15.5 ± 0.66	22.5 ± 1.91	9.2 ± 0.11
17	10f	5-CHO-2-thiophenyl	3.6 ± 0.31	8.2 ± 0.11	16.6 ± 0.21	13.9 ± 0.22
18	10g	3,4-Methylenedioxy-Ph	6.7 ± 0.16	16.3 ± 1.25	30.2 ± 1.34	19.6 ± 0.20
19	10h	2,3-Cl-Ph	9.9 ± 0.12	14.0 ± 0.35	27.6 ± 1.06	10.5 ± 0.63
20	10i	3-Furyl	52.7 ± 1.93	91.2 ± 7.33	126.0 ± 3.18	62.8 ± 1.76
21	10j	2,4-OMePh	71.7 ± 7.27	62.7 ± 5.83	100.6 ± 7.61	69.1 ± 6.64
22	10k	4-CHO-Ph	11.1 ± 0.15	18.2 ± 1.82	36.2 ± 1.36	12.7 ± 0.19
23	10l	4-CN-Ph	13.61 ± 0.61	11.6 ± 0.40	25.4 ± 2.13	16.6 ± 0.64
24	10m	4-OMe-Ph	45.4 ± 5.14	55.7 ± 0.47	98.0 ± 0.70	61.7 ± 8.30
25	10n	3-Cl,4-Me-Ph	7.4 ± 0.14	12.1 ± 1.19	21.1 ± 0.91	10.4 ± 0.04
27	10o	4-SMe-Ph	15.8 ± 0.37	26.4 ± 4.27	50.4 ± 0.27	18.7 ± 0.20
28	Doxorubicin	–	1.6 ± 0.08	0.95 ± 0.20	1.9 ± 0.12	1.4 ± 0.27
29	Tamoxifen	–	8.0 ± 0.20	19.3 ± 0.79	24.4 ± 0.26	21.7 ± 0.97

GI₅₀ values represent as mean ± SD of three determinations.

[14]. Mitochondrial changes, including loss of mitochondrial membrane potential ($\Delta\Psi_m$), are key events that take place during drug-induced apoptosis. Mitochondrial injury by **9b** and **9e** was evaluated by detecting drops in mitochondrial membrane potential ($\Delta\Psi_m$). In this study, we have investigated the involvement of mitochondria in the induction of apoptosis by these compounds. After 48 h of treatment with compounds **9b** and **9e**, reduction in mitochondrial membrane potential ($\Delta\Psi_m$) of MCF-7 cells was observed, that was assessed by JC-1 staining [Fig. 3].

2.2.4. Effect on intracellular ROS generation

Many anticancer agents have demonstrated to exert their cytotoxic effects by the generation of reactive oxygen species (ROS) [15], which is considered as one of the key mediators of apoptotic signaling. Therefore, we decided to investigate the role of compounds **9b** and **9e** in inducing the production of ROS that could potentially lead to the cytotoxic effect in the MCF-7 cells. In order to demonstrate the role of compounds on ROS generation during apoptosis process, production of ROS was examined by using an oxidant-sensitive fluorescent probe, DCFDA (2',7'-dichlorofluoresceindiacetate). After treatment with compounds **9b** and **9e** at 0.5 and 1 μM concentrations for 48 h, the level of ROS was significantly increased [Fig. 4]. The ratio of DCF-positive cells for compounds **9b** and **9e** was 30.4 and 16.2% and 78.5 and 57.4% respectively at 0.5 and 1 μM concentrations for 48 h. Untreated control cells showed only 1.2% DCF positive cells. The results confirmed that these compounds had enhanced the generation of ROS in MCF-7 cells.

2.2.5. Annexin V-FITC for apoptosis

The apoptotic effects of **9b** and **9e** were further evaluated by Annexin V FITC/PI (AV/PI) dual staining assay [16] to examine the occurrence of phosphatidylserine externalization and also to understand whether it is due to physiological apoptosis or nonspecific necrosis. In this study MCF-7 cells were treated with compounds **9b** and **9e** for 48 h at 0.5 and 1 μM concentrations to examine the apoptotic effect. It was observed that these compounds showed

significant apoptosis against MCF-7 cells as shown in Fig. 5 and Table 3. Results indicated that compounds **9b** and **9e** showed 12.63 and 11.47% and 39.0 and 30.85% apoptosis respectively at 0.5 and 1 μM concentrations for 48 h.

2.2.6. Activation of caspase-9

The activation of caspases plays an important role in the process of programmed cell death or apoptosis. Caspases or cysteine-specific proteases are crucial mediators of apoptosis. The MCF-7 cells lack endogenous caspase-3, whereas caspase-9 plays an important role in mediating drug-induced apoptosis [17]. MCF-7 cells were treated with compounds **9b** and **9e** at 1 μM concentration for 48 h. The results demonstrate that there was 2–3 fold induction in caspase-9 activity when compared to untreated control [Fig. 6] which suggested that they have the ability to induce cell death by apoptosis in MCF-7 cells.

2.2.7. Western blot analysis of Bcl-2, Bax, p53, p21 and p27

The members of the Bcl-2 family play a pivotal role in the regulation of the mitochondrial apoptotic pathway. Among these, Bcl-2 inhibits apoptosis, whereas Bax counterbalances the Bcl 2 effect and stimulates apoptosis [18]. Activation of tumor suppressor genes such as p53 and p27 is found to be important in the regulation of apoptotic pathway induced by various stimuli [19]. The p53 gene, is a tumor suppressor gene and its activity stops the formation of tumors. p27 is considered the main regulator of G1 phase activity, and p21 function as a sensor of cytostatic signals and is mainly regulated by the p53 tumor suppressor gene [20]. In the cell cycle study, we observed that these compounds caused cell cycle arrest at G1 phase. To further evidence the expression of possible G1 cell cycle-associated regulators (p53, p21 and p27) along with proapoptotic protein bax and anti-apoptotic protein bcl-2 were detected by western blot analysis. As shown in Fig. 7, we observed that compounds **9b** and **9e** induced G1 cell cycle arrest in MCF-7 cells might be through induction of p53, p21, p27 and bax followed by a decrease in the expression of Bcl-2.

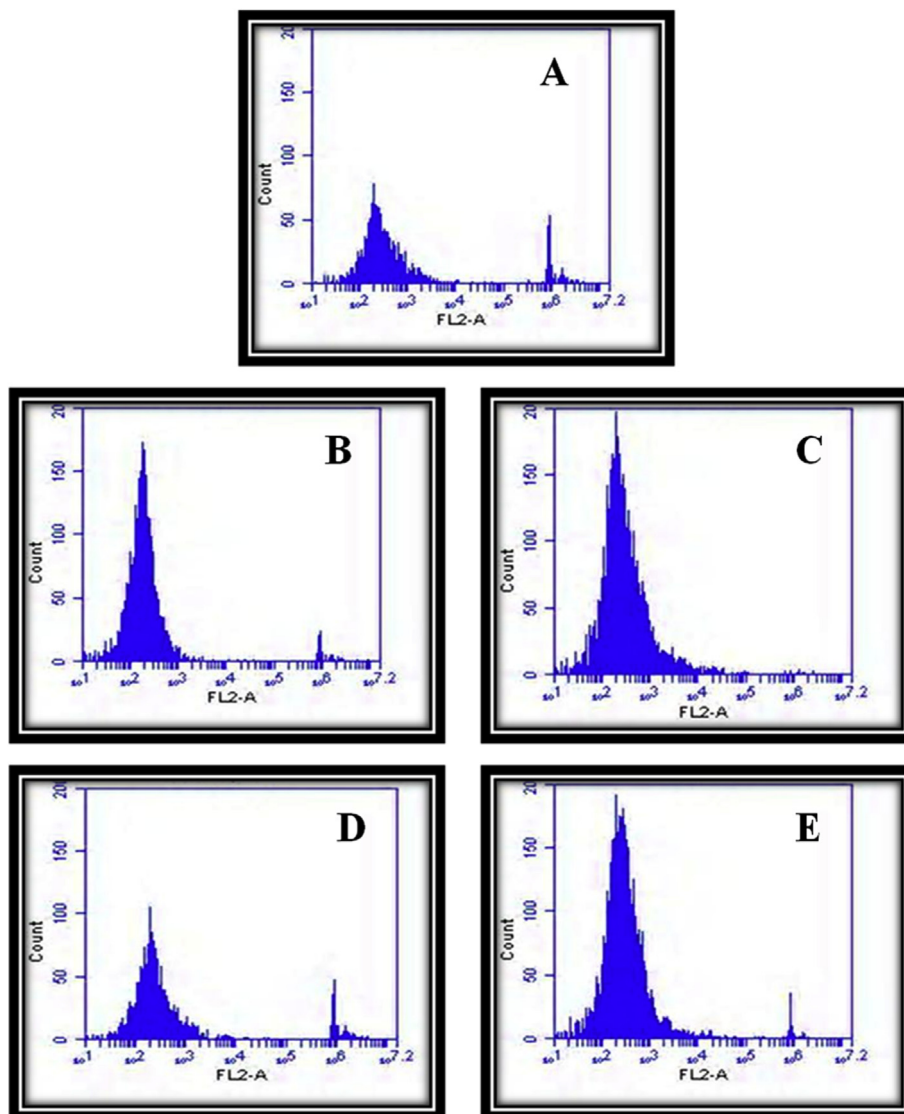


Fig. 2. Flow cytometric analysis in MCF-7 breast cancer cell lines after treatment with compounds. A: Control cells (MCF-7), B: **9b** (0.5 μ M), C: **9b** (1 μ M), D: **9e** (0.5 μ M) and E: **9e** (1 μ M).

Table 2
Effect of compounds **9b** and **9e** on cell-cycle phase distribution in MCF-7 cells.

Sample	Sub G1%	G0/G1%	S %	G2/M %
A: Control (MCF-7)	2.75	77.79	0.99	11.98
B: 9b (0.5 μ M)	4.38	84.21	0.34	3.35
C: 9b (1 μ M)	3.69	89.15	1.75	0.76
D: 9e (0.5 μ M)	2.89	81.44	1.12	9.63
E: 9e (1 μ M)	3.25	88.42	1.30	2.20

3. Conclusions

In summary, we have discovered oxa/azaspiro[4,5]trienones as novel scaffolds for anticancer drug development. The synthesis is straightforward and high yielding. The biological studies revealed that these compounds cause cell cycle arrest at G0/G1 phase and induced mitochondria mediated apoptosis. Studies like, measurement of mitochondrial membrane potential, ROS generation, Caspase 9 activity, Annexin V-FITC assay and western blot analysis demonstrated that these compounds disrupt mitochondrial potential by increasing ROS production in order to induce apoptosis.

Considering the better growth inhibition shown by oxaspiro[4,5]trienones over azaspiro[4,5]trienones, it was inferred that a lipophilic replacement of oxygen might improve the anticancer potential of these scaffolds. Hit optimization with various possible derivatives of spiro[4,5]trienones is currently underway and will be reported in due course.

3.1. Experimental

3.1.1. General

Compound **6** and **7** were synthesized from commercially available chemicals using previously reported procedures. Reagents and solvents were purchased from locally available commercial suppliers and were used without further purification. ^1H and ^{13}C NMR spectra were obtained on Bruker DRX-300 and Avance-500. Chemical shifts were reported in ppm on the basis of a comparison with tetramethylsilane (TMS) as an internal standard or residual solvent peak (for ^1H NMR spectra, CDCl_3 : 7.26 and for ^{13}C NMR spectra, CDCl_3 : 77.16). Multiplicity was indicated as follows: s (singlet); d (doublet); t (triplet); q (quartet); m (multiplet); dd

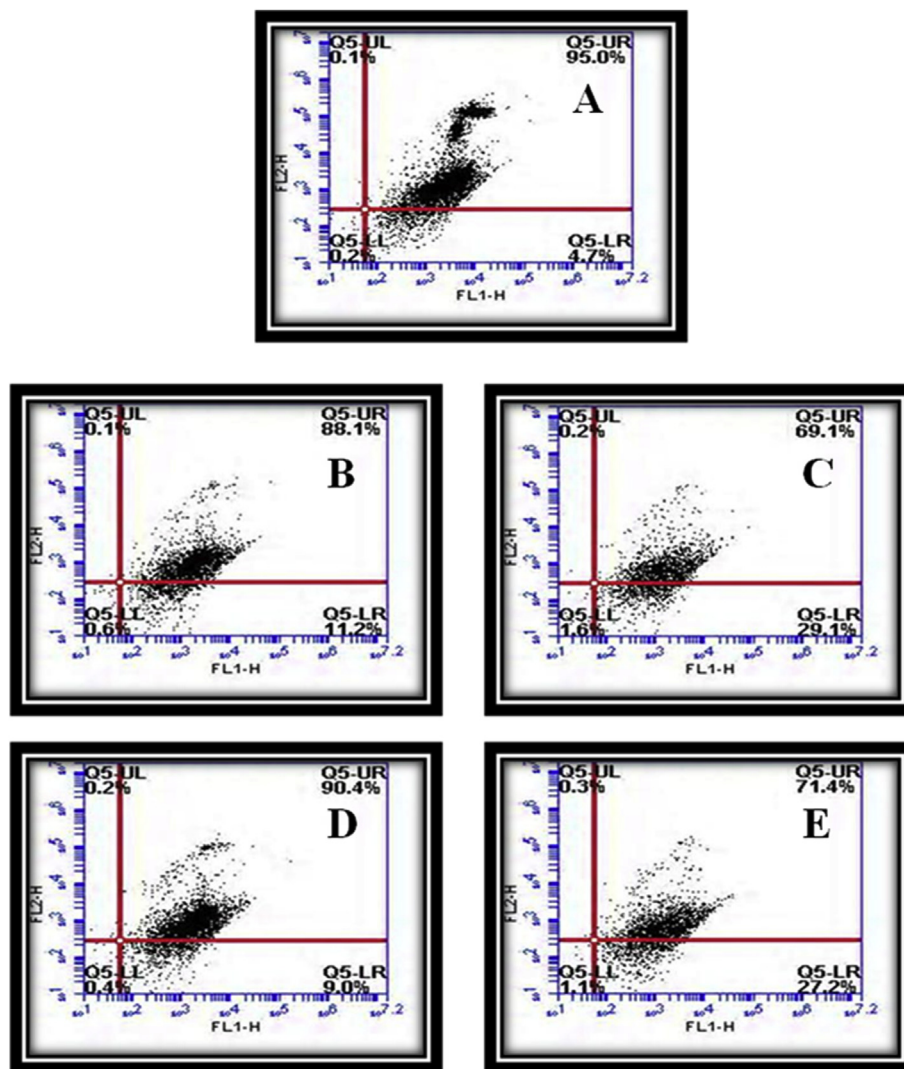


Fig. 3. Compounds **9b** and **9e** triggers mitochondrial injury. Drops in membrane potential ($\Delta\Psi_m$) was assessed by JC-1 staining of MCF-7 cells treated with test compound and samples were then subjected to flow cytometry analysis on a FACScan (Becton Dickinson) in the FL1, FL2 channel to detect mitochondrial potential. A: Control cells (MCF-7), B: **9b** (0.5 μ M), C: **9b** (1 μ M), D: **9e** (0.5 μ M) and E: **9e** (1 μ M).

(doublet of doublet), bs (broad singlet), etc., and coupling constants are given in hertz (Hz). The low-resolution mass spectrometric analysis was performed at National Center for Mass Spectrometry, CSIR–IICT. The conversion of starting materials was monitored by thin layer chromatography (TLC) using silica gel plates (silica gel 60 F₂₅₄ 0.25 mm), and the reaction components were visualized by observation under UV light (254 and 365 nm) or by treatment of TLC plates with visualizing agents such as KMnO₄, anisaldehyde and ceric sulfate which was followed by heating. All reactions were carried out in oven-dried glassware or 20 mL vials with silicon caps. Products were purified by column chromatography on silica gel (100–200 mesh) using a mixture of EtOAc/hexane or MeOH/DCM as eluents.

3.1.2. Methyl (E)-3-(2,8-dioxo-4-phenyl-1-oxaspiro[4.5]deca-3,6,9-trien-3-yl)acrylate **9h**

To a solution of Compound **6** (200 mg, 0.549 mmol) in DMF (4 mL), Pd(OAc)₂ (0.0005 mmol) was added, and K₂CO₃ (152 mg, 1.09 mmol) was added, followed by methyl acrylate (110 μ L, 1.09 mmol) was added and the mixture was stirred under reflux at 80 °C. The reaction progress was monitored by TLC. After completion of the reaction, the mixture was allowed to cool at room

temperature and reaction mixture dissolve in Ethylacetate (5 mL), then crushed ice was added to the mixture, compound was extracted with ethylacetate (3 \times 30 mL). The organic layers were collected, combined, washed with saturated aq NaCl (2 \times 25 mL), dried over anhydrous Na₂SO₄, filtered and concentrated under reduced pressure. The crude compound was purified by column chromatography on silica gel to afford **9h** (132 mg). Yield = 74%; R_f = 0.43 (30% EtOAc in hexane); ¹H NMR (500 MHz, CDCl₃) δ 7.51–7.47 (m, 1H), 7.43 (td, *J* = 1.37 Hz, 2H), 7.27 (d, *J* = 1.52 Hz, 1H), 7.27 (s, 1H), 7.24 (d, *J* = 8.08 Hz, 2H), 6.65 (dt, *J* = 1.83, 2.89 Hz, 2H), 6.40 (dd, *J* = 1.67, 10.07 Hz, 2H), 3.77 (s, 3H), ¹³C NMR (125 MHz, CDCl₃) δ 183.5, 168.9, 166.8, 163.7, 142.0, 132.1, 131.2, 130.9, 129.2, 128.8, 128.0, 125.9, 124.1, 81.2, 52.0; ESIMS (*m/z*): calcd for C₁₉H₁₄O₅ = 322, found [M+H]⁺ = 323.

3.1.3. General procedure for the Suzuki coupling

To a solution of compound **6** or **7** (0.274 mmol) in DMF (4 mL) and water (1 mL) was added Pd(OAc)₂ (6 mg, 0.027 mmol), then boronic acid **8** (0.548 mmol) and K₂CO₃ (75.6 mg, 0.548 mmol) and the mixture was stirred under reflux at 85 °C. The reaction progress was monitored by TLC. After completion of the reaction, the mixture was allowed to cool at room temperature and the mixture

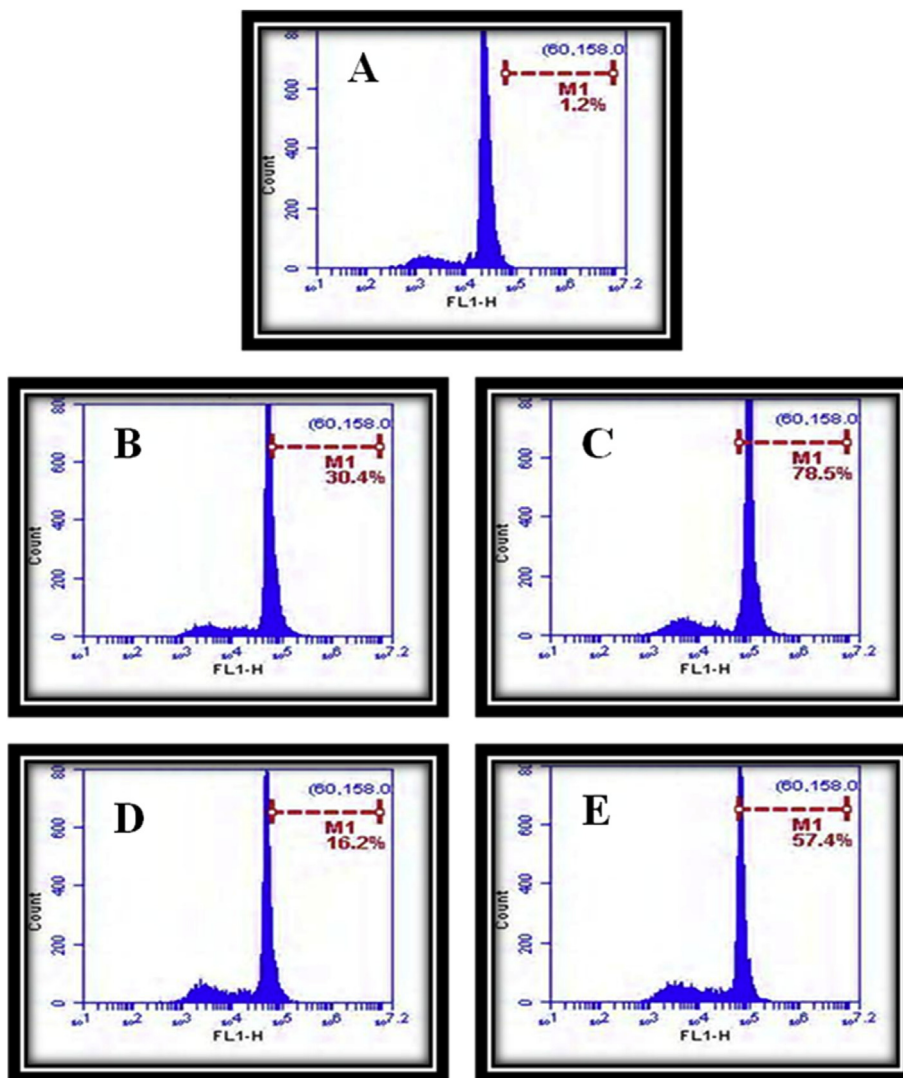


Fig. 4. The effect of **9b** and **9e** on the ROS production in human breast cancer cells (MCF-7). A: Control cells (MCF-7), B: **9b** (0.5 μ M), C: **9b** (1 μ M), D: **9e** (0.5 μ M) and E: **9e** (1 μ M).

was extracted with ethylacetate (3×30 mL). The organic layers were collected, combined, washed with saturated aq NaCl (2×25 mL), dried over anhydrous Na_2SO_4 , filtered and concentrated under reduced pressure. The crude compound was purified by column chromatography on silica gel to afford the coupled product.

3.1.4. 3-(4-(Hydroxymethyl)phenyl)-1-methyl-4-phenyl-1-azaspiro [4.5]deca-3,6,9-triene-2,8-dione **10a**

Yield = 71.3%; R_f = 0.29 (30% EtOAc in hexane); ^1H NMR (300 MHz, $\text{DMSO}-d_6$) δ 7.39 (d, J = 8.30 Hz, 2H), 7.31–7.27 (m, 2H), 7.23–7.20 (m, 3H), 7.10 (dd, J = 1.51, 8.30 Hz, 2H), 6.59 (d, J = 10.19 Hz, 2H), 6.47 (d, J = 10.19 Hz, 2H), 4.62 (s, 2H), 2.95 (s, 3H); ^{13}C NMR (75 MHz, CDCl_3 & $\text{DMSO}-d_6$) δ 183.3, 168.8, 148.8, 145.1, 141.9, 134.5, 132.3, 131.1, 128.6, 128.6, 128.4, 127.9, 127.7, 125.7, 66.4, 29.3; HRMS (ESI) calcd for $\text{C}_{23}\text{H}_{20}\text{NO}_3$ $[\text{M}+\text{H}]^+$ = 358.1443, found = 358.1445.

3.1.5. 3-(Benzo[b]thiophen-2-yl)-1-methyl-4-phenyl-1-azaspiro [4.5]deca-3,6,9-triene-2,8-dione **10b**

Yield = 79.2%; R_f = 0.31 (30% EtOAc in hexane); ^1H NMR (500 MHz, CDCl_3) δ 8.14 (s, 1H), 7.73 (dd, J = 1.83, 5.95 Hz, 1H), 7.66–7.64 (m, 1H), 7.48–7.44 (m, 1H), 7.41–7.38 (m, 2H), 7.31–7.27

(m, 2H), 7.17 (dd, J = 1.06, 8.08 Hz, 2H), 6.59 (d, J = 10.22 Hz, 2H), 6.44 (d, J = 10.22 Hz, 2H), 3.02 (s, 3H); ^{13}C NMR (125 MHz, CDCl_3) δ 183.8, 168.5, 148.0, 144.9, 140.2, 138.7, 133.3, 132.3, 130.8, 129.8, 128.9, 128.8, 126.3, 125.3, 124.3, 124.3, 121.8, 67.5, 29.6; HRMS (ESI) calcd for $\text{C}_{24}\text{H}_{18}\text{NO}_2\text{S}$ $[\text{M}+\text{H}]^+$ = 384.1058, found = 384.1060; HPLC purity = 94.09%.

3.1.6. 1-Methyl-4-phenyl-3-(4-(trifluoromethyl)phenyl)-1-azaspiro [4.5]deca-3,6,9-triene-2,8-dione **10c**

Yield = 78%; R_f = 0.37 (30% EtOAc in hexane); ^1H NMR (500 MHz, CDCl_3) δ 7.70 (s, 1H), 7.60 (d, J = 7.78 Hz, 1H), 7.52 (d, J = 7.78 Hz, 1H), 7.38 (t, J = 7.78 Hz, 1H), 7.33 (tt, J = 1.22, 2.89 Hz, 1H), 7.28 (d, J = 7.62 Hz, 2H), 7.10 (d, J = 7.17 Hz, 2H), 6.60 (dt, J = 1.98, 2.74 Hz, 2H), 6.51 (dt, J = 1.98, 2.74 Hz, 2H), 2.98 (s, 3H); ^{13}C NMR (75 MHz, CDCl_3) δ 184.0, 169.1, 151.5, 145.0, 138.9, 133.4, 132.6, 131.2, 131.0, 129.7, 128.8, 128.7, 128.2, 126.4, 126.3, 125.3, 125.3, 67.2, 29.6; HRMS (ESI) calcd for $\text{C}_{23}\text{H}_{17}\text{F}_3\text{NO}_2$ $[\text{M}+\text{H}]^+$ = 396.1211, found = 396.1213; HPLC purity = 97.33%.

3.1.7. 1-Methyl-3-(naphthalen-1-yl)-4-phenyl-1-azaspiro[4.5]deca-3,6,9-triene-2,8-dione **10d**

Yield = 63.7%; R_f = 0.31 (30% EtOAc in hexane); ^1H NMR (500 MHz, CDCl_3) δ 7.84 (d, J = 8.24 Hz, 1H), 7.67 (d, J = 8.39, 1H),

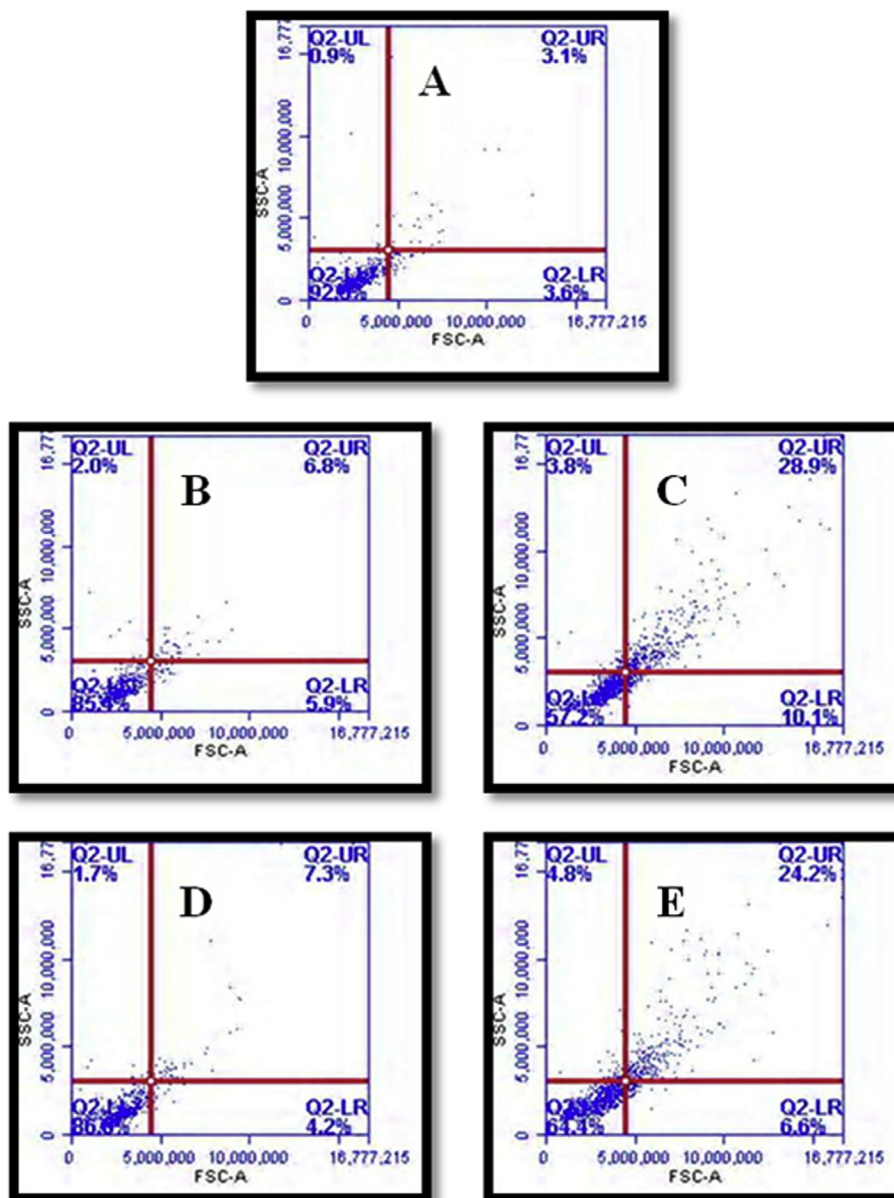


Fig. 5. Annexin V-FITC staining. A: Control cells (MCF-7), B: **9b** (0.5 μ M), C: **9b** (1 μ M), D: **9e** (0.5 μ M) and E: **9e** (1 μ M).

7.46–7.42 (m, 2H), 7.41–7.37 (m, 1H), 7.35 (dd, $J = 1.22, 7.01$ Hz, 1H), 7.13 (tt, $J = 1.37, 1.98$ Hz, 1H), 7.09 (d, $J = 6.86$ Hz, 2H), 7.03 (t, $J = 7.93$ Hz, 2H), 6.78 (dd, $J = 3.20, 10.22$ Hz, 2H), 6.74 (dd, $J = 3.05, 10.22$ Hz, 2H), 6.61–6.58 (m, 2H), 3.00 (s, 3H); ^{13}C NMR (75 MHz, CDCl_3) δ 184.2, 169.9, 151.8, 146.3, 145.9, 133.7, 133.1, 131.3, 131.0, 129.4, 129.3, 128.6, 128.4, 128.2, 127.8, 126.3, 126.0, 125.4, 124.9, 67.0, 29.7; HRMS (ESI) calcd for $\text{C}_{26}\text{H}_{20}\text{NO}_2$ $[\text{M}+\text{H}]^+ = 378.1494$, found = 378.1496.

Table 3
Distribution of apoptotic cells in Annexin-V FITC experiment.

Sample	UL %	UR %	LL%	LR%
A: Control	0.86	3.08	92.50	3.57
B: 9b (0.5 μ M)	1.96	6.76	85.41	5.87
C: 9b (1 μ M)	3.77	28.87	57.24	10.13
D: 9e (0.5 μ M)	1.69	7.25	86.85	4.22
E: 9e (1 μ M)	4.77	24.21	64.39	6.64

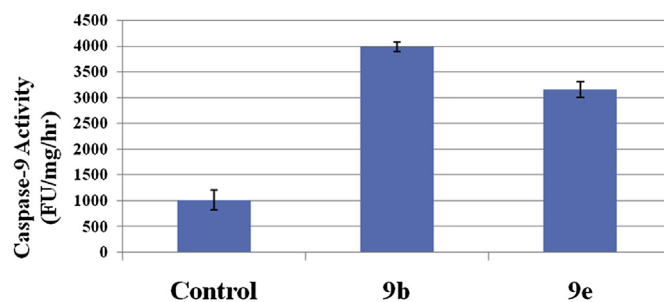


Fig. 6. Effect of compounds **9b** and **9e** on caspase-9 activity; MCF-7 breast cancer cells were treated with these compounds at 1 μ M concentration for 48 h. Values indicated are the mean \pm SD of two different experiments performed in triplicates.

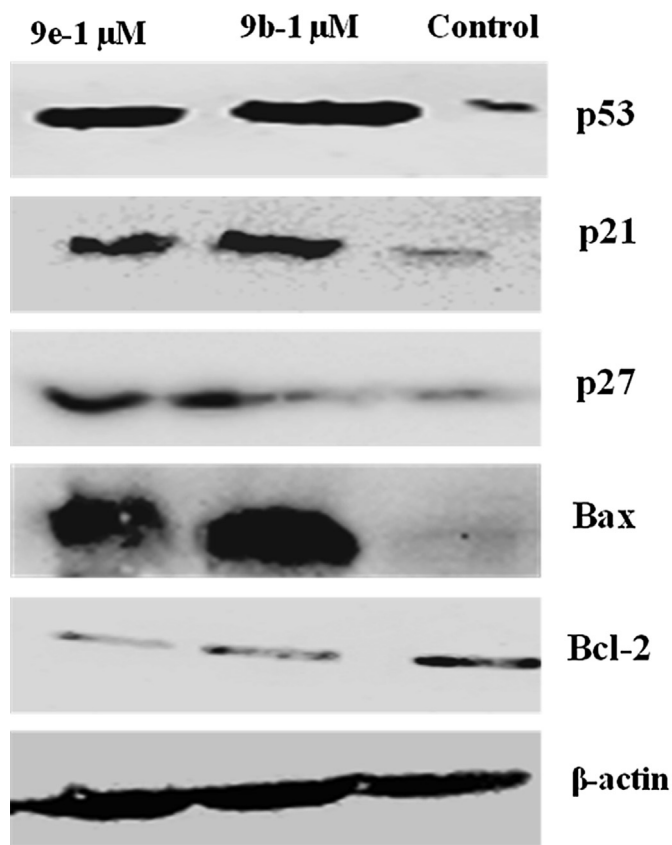


Fig. 7. The effect of compounds on p53, p21, p27, Bax and Bcl-2 levels: MCF-7 cells were treated with compounds **9b** and **9e** at 1 μ M concentration for 48 h. Cell lysates were collected, and the expression levels of p53, p21, p27, Bax and Bcl-2 were determined by western blot analysis. β -Actin was used as a loading control.

3.1.8. 1-Methyl-3,4-diphenyl-1-azaspiro[4.5]deca-3,6,9-triene-2,8-dione **10e**

Yield = 64.9%; R_f = 0.31 (30% EtOAc in hexane); ^1H NMR (500 MHz, CDCl_3) δ 7.42–7.40 (m, 2H), 7.31–7.27 (m, 3H), 7.23 (t, J = 7.62 Hz, 2H), 7.11 (d, J = 7.17 Hz, 2H), 6.60 (d, J = 10.07 Hz, 2H), 6.48 (d, J = 10.22 Hz, 2H), 2.96 (s, 3H); ^{13}C NMR (75 MHz, CDCl_3) δ 184.2, 169.6, 149.7, 145.7, 135.6, 133.2, 132.7, 130.5, 129.4, 129.3, 128.6, 128.4, 128.2, 128.0, 67.0, 29.7; HRMS (ESI) calcd for $\text{C}_{22}\text{H}_{18}\text{NO}_2$ $[\text{M}+\text{H}]^+$ = 328.1338, found = 328.1335; HPLC purity = 98.60%.

3.1.9. 5-(1-Methyl-2,8-dioxo-4-phenyl-1-azaspiro[4.5]deca-3,6,9-trien-3-yl)thiophene-2-carbaldehyde **10f**

Yield = 73.8%; R_f = 0.21 (30% EtOAc in hexane); ^1H NMR (500 MHz, CDCl_3) δ 9.84 (s, 1H), 7.63 (d, J = 4.12 Hz, 1H), 7.56 (d, J = 4.12 Hz, 1H), 7.46 (tt, J = 1.37, 2.74 Hz, 1H), 7.41 (tt, J = 1.37, 1.98 Hz, 2H), 7.12 (dt, J = 1.98 Hz, 2H), 6.56 (dt, J = 1.98, 2.74 Hz, 2H), 6.45 (dt, J = 1.98, 2.74 Hz, 2H), 3.00 (s, 3H); ^{13}C NMR (125 MHz, CDCl_3) δ 187.3, 183.2, 168.8, 144.1, 135.3, 133.6, 130.2, 129.4, 129.2, 129.1, 128.1, 67.7, 26.5; HRMS (ESI) calcd for $\text{C}_{21}\text{H}_{16}\text{NO}_3\text{S}$ $[\text{M}+\text{H}]^+$ = 362.0851, found = 362.0850; HPLC purity = 79.78%.

3.1.10. 3-(Benzo[d][1,3]dioxol-5-yl)-1-methyl-4-phenyl-1-azaspiro[4.5]deca-3,6,9-triene-2,8-dione **10g**

Yield = 68%; R_f = 0.28 (30% EtOAc in hexane); ^1H NMR (500 MHz, CDCl_3) δ 7.30–7.24 (m, 3H), 7.12 (d, J = 7.62 Hz, 2H), 6.97 (d, J = 8.24 Hz, 1H), 6.90 (s, 1H), 6.70 (d, J = 8.24 Hz, 1H), 6.57 (d, J = 8.54 Hz, 2H), 6.46 (d, J = 9.00 Hz, 2H), 5.92 (s, 2H), 2.95 (s, 3H);

^{13}C NMR (100 MHz, CDCl_3) δ 184.0, 169.5, 148.4, 147.8, 147.3, 145.6, 134.6, 133.0, 131.8, 129.1, 128.6, 128.2, 124.1, 123.8, 109.6, 108.1, 101.0, 66.8, 26.1; HRMS (ESI) calcd for $\text{C}_{23}\text{H}_{18}\text{NO}_4$ $[\text{M}+\text{H}]^+$ = 372.1236, found = 372.1240; HPLC purity = 93.13%.

3.1.11. 3-(2,3-Dichlorophenyl)-1-methyl-4-phenyl-1-azaspiro[4.5]deca-3,6,9-triene-2,8-dione **10h**

Yield = 68.6%; R_f = 0.28 (30% EtOAc in hexane); ^1H NMR (500 MHz, CDCl_3) δ 7.45 (dd, J = 1.52, 7.93 Hz, 1H), 7.28 (dt, J = 1.22, 1.98 Hz, 1H), 7.21–7.17 (m, 3H), 7.11 (dq, J = 1.52 Hz, 3H), 6.65 (dd, J = 1.67, 10.22 Hz, 2H), 6.58–6.53 (m, 2H), 2.95 (s, 3H); ^{13}C NMR (100 MHz, CDCl_3) δ 183.9, 168.4, 152.4, 145.5, 144.9, 135.1, 133.5, 133.3, 133.0, 132.7, 131.9, 130.8, 130.7, 129.7, 129.4, 128.5, 127.5, 127.4, 67.0, 26.0; HRMS (ESI) calcd for $\text{C}_{22}\text{H}_{16}\text{Cl}_2\text{NO}_2$ $[\text{M}+\text{H}]^+$ = 396.0558, found = 396.0563; HPLC purity = 98.50%.

3.1.12. 3-(Furan-3-yl)-1-methyl-4-phenyl-1-azaspiro[4.5]deca-3,6,9-triene-2,8-dione **10i**

Yield = 83.3%; R_f = 0.40 (30% EtOAc in hexane); ^1H NMR (500 MHz, CDCl_3) δ 8.28 (q, J = 0.76 Hz, 1H), 7.41–7.34 (m, 3H), 7.22 (t, J = 1.67 Hz, 1H), 7.14 (dt, J = 1.37 Hz, 2H), 6.55 (dt, J = 1.98, 2.74 Hz, 2H), 6.42 (d, J = 1.98, 2.74 Hz, 2H), 5.85 (dd, J = 0.76, 1.98 Hz, 1H), 2.96 (s, 3H); ^{13}C NMR (125 MHz, CDCl_3) δ 169.4, 145.9, 145.3, 143.7, 142.4, 133.1, 131.7, 129.3, 128.7, 128.4, 108.5, 67.7, 29.6; HRMS (ESI) calcd for $\text{C}_{20}\text{H}_{16}\text{NO}_3$ $[\text{M}+\text{H}]^+$ = 318.1130, found = 318.1131; HPLC purity = 97.35%.

3.1.13. 3-(2,4-Dimethoxyphenyl)-1-methyl-4-phenyl-1-azaspiro[4.5]deca-3,6,9-triene-2,8-dione **10j**

Yield = 69.3%; R_f = 0.18 (30% EtOAc in hexane); ^1H NMR (500 MHz, CDCl_3) δ 7.29 (d, J = 8.39 Hz, 1H), 7.23–7.20 (m, 1H), 7.16 (t, J = 7.78, 2H), 7.13 (d, J = 7.17 Hz, 2H), 6.63 (d, J = 9.91 Hz, 2H), 6.52–6.49 (m, 3H), 6.34 (d, J = 2.28 Hz, 1H), 3.80 (s, 3H), 3.37 (s, 3H), 2.93 (s, 3H); ^{13}C NMR (125 MHz, CDCl_3) δ 173.9, 161.4, 157.9, 133.2, 132.7, 131.7, 131.5, 128.9, 128.2, 127.2, 112.9, 111.7, 104.5, 98.9, 55.3, 54.8, 29.7; HRMS (ESI) calcd for $\text{C}_{24}\text{H}_{22}\text{NO}_4$ $[\text{M}+\text{H}]^+$ = 388.1549, found = 388.1548; HPLC purity = 97.79%.

3.1.14. 4-(1-Methyl-2,8-dioxo-4-phenyl-1-azaspiro[4.5]deca-3,6,9-trien-3-yl)benzaldehyde **10k**

Yield = 70.2%; R_f = 0.18 (30% EtOAc in hexane); ^1H NMR (500 MHz, CDCl_3) δ 9.97 (d, J = 3.66 Hz, 1H), 7.77 (dt, J = 1.67 Hz, 2H), 7.59 (dd, J = 2.13, 8.39 Hz, 2H), 7.35–7.31 (m, 1H), 7.26 (t, J = 7.62 Hz, 2H), 7.10 (d, J = 8.54 Hz, 2H), 6.60 (dd, J = 2.59, 12.66 Hz, 2H), 6.50 (dt, J = 2.74 Hz, 2H), 2.98 (s, 3H); ^{13}C NMR (75 MHz, CDCl_3) δ 191.8, 183.9, 168.9, 152.1, 145.0, 136.6, 135.8, 134.4, 133.4, 131.2, 130.1, 129.8, 129.4, 128.9, 128.2, 67.1, 29.6; HRMS (ESI) calcd for $\text{C}_{23}\text{H}_{18}\text{NO}_3$ $[\text{M}+\text{H}]^+$ = 356.1287, found = 356.1288; HPLC purity = 96.35%.

3.1.15. 4-(1-Methyl-2,8-dioxo-4-phenyl-1-azaspiro[4.5]deca-3,6,9-trien-3-yl)benzotrile **10l**

Yield = 72.1%; R_f = 0.33 (30% EtOAc in hexane); ^1H NMR (300 MHz, CDCl_3) δ 7.54 (s, 4H), 7.35 (t, J = 7.62 Hz, 1H), 7.29 (d, J = 7.62 Hz, 2H), 7.08 (d, J = 7.32 Hz, 2H), 6.58 (d, J = 10.22 Hz, 2H), 6.51 (d, J = 10.22 Hz, 2H), 2.97 (s, 3H); ^{13}C NMR (125 MHz, CDCl_3) δ 183.9, 168.8, 152.6, 144.8, 135.3, 133.8, 133.7, 132.0, 131.1, 130.2, 130.0, 129.1, 128.3, 118.6, 112.3, 67.3, 29.8; HRMS (ESI) calcd for $\text{C}_{23}\text{H}_{17}\text{N}_2\text{O}_2$ $[\text{M}+\text{H}]^+$ = 353.1290, found = 353.1290; HPLC purity = 94.26%.

3.1.16. 3-(4-Methoxyphenyl)-1-methyl-4-phenyl-1-azaspiro[4.5]deca-3,6,9-triene-2,8-dione **10m**

Yield = 78.5%; R_f = 0.25 (30% EtOAc in hexane); ^1H NMR (500 MHz, CDCl_3) δ 7.39 (dd, J = 2.74, 11.59 Hz, 2H), 7.31–7.23 (m, 3H), 7.12 (d, J = 7.17 Hz, 2H), 6.78 (dd, J = 2.74, 11.59 Hz, 2H), 6.59

(dd, $J = 2.59, 12.66$ Hz, 2H), 6.47 (dd, $J = 2.59, 12.66$ Hz, 2H), 3.77 (s, 3H), 2.96 (s, 3H); ^{13}C NMR (125 MHz, CDCl_3) δ 184.2, 169.8, 159.7, 147.7, 145.9, 134.6, 133.0, 132.1, 130.8, 129.0, 128.6, 128.3, 122.9, 113.6, 66.9, 55.1, 29.6; HRMS (ESI) calcd for $\text{C}_{23}\text{H}_{20}\text{NO}_3$ $[\text{M}+\text{H}]^+ = 358.1443$, found = 358.1443; HPLC purity = 99.53%.

3.1.17. 3-(3-Chloro-4-methylphenyl)-1-methyl-4-phenyl-1-azaspiro[4.5]deca-3,6,9-triene-2,8-dione **10n**

Yield = 71.1%; $R_f = 0.37$ (30% EtOAc in hexane); ^1H NMR (500 MHz, CDCl_3) δ 7.48 (d, $J = 1.67$ Hz, 1H), 7.32 (tt, $J = 1.37, 2.28$ Hz, 1H), 7.28–7.24 (m, 2H), 7.15 (dd, $J = 1.67, 7.93$ Hz, 1H), 7.12–7.08 (m, 3H), 6.58 (dt, $J = 1.98, 2.74$ Hz, 2H), 6.48 (dt, $J = 1.98, 2.74$ Hz, 2H), 2.96 (s, 3H), 2.32 (s, 3H); ^{13}C NMR (125 MHz, CDCl_3) δ 184.0, 169.2, 150.0, 145.4, 136.9, 134.2, 134.0, 133.2, 131.4, 130.6, 129.7, 129.5, 129.4, 128.7, 128.2, 127.5, 67.0, 29.6, 19.9; HRMS (ESI) calcd for $\text{C}_{23}\text{H}_{19}\text{ClNO}_2$ $[\text{M}+\text{H}]^+ = 376.1104$, found = 376.1105; HPLC purity = 98.89%.

3.1.18. 1-Methyl-3-(4-(methylthio)phenyl)-4-phenyl-1-azaspiro[4.5]deca-3,6,9-triene-2,8-dione **10o**

Yield = 70.7%; $R_f = 0.25$ (30% EtOAc in hexane); ^1H NMR (500 MHz, CDCl_3) δ 7.36 (d, $J = 8.54$ Hz, 2H), 7.30 (t, $J = 7.62$ Hz, 1H), 7.25 (d, $J = 7.93$ Hz, 2H), 7.12–7.10 (m, 4H), 6.58 (d, $J = 9.91$ Hz, 2H), 6.47 (d, $J = 10.07$ Hz, 2H), 2.96 (s, 3H), 2.44 (s, 3H); ^{13}C NMR (125 MHz, CDCl_3) δ 184.0, 169.5, 148.9, 145.6, 139.6, 134.6, 133.1, 131.8, 129.6, 129.2, 128.6, 128.3, 126.9, 125.5, 66.9, 29.6, 15.1; HPLC purity = 99.17%.

3.1.19. In vitro anti-proliferative assay

The anti-proliferative activities of the compounds were calculated from the growth inhibition data at three different concentrations (1, 5 and 10 μM) by using Sulphorhodamine B (SRB) assay [15]. Cells grown in DMEM, supplemented with 10% FBS were seeded in each well of 96 well microculture plates and incubated for 24 h at 37 °C in a CO_2 incubator. Compounds, diluted to the desired concentrations (1, 5 and 10 μM) in DMSO, were added to the wells. All the working solutions were prepared from stock solution of DMSO (10 mM). The maximum concentration of DMSO used for the assay was 0.1%. After 48 h, cells were fixed with 10% trichloroacetic acid (TCA) solution and were further incubated for 60 min at 4 °C. The plates were washed with tap water and air dried. Later Sulforhodamine B (SRB) solution (50 μl) at 0.4% (w/v) in 1% acetic acid was added to each well, and plates were incubated for 20 min at room temperature. The residual dye was removed by washing with 1% acetic acid and the plates were air dried. Bound stain was subsequently eluted with 10 mM Tris base, and the absorbance was recorded on multimode reader (TECAN) at a wavelength of 540 nm. All experiments were performed in triplicate.

3.1.20. Cell cycle analysis

Flow cytometric analysis (FACS) was performed to evaluate the distribution of the cells through the cell-cycle phases. MCF-7 cells, breast cancer cells were incubated for 48 h with compounds **9b** and **9e** at concentrations of 0.5 and 1 μM . Untreated and treated cells were harvested, washed with phosphate-buffered saline (PBS), fixed in ice-cold 70% ethanol, and stained with propidium iodide (Sigma–Aldrich). Cell-cycle analysis was performed by flow cytometry (Becton Dickinson FACS Caliber instrument) [16].

3.1.21. Mitochondrial membrane potential

MCF-7 (1×10^6 cells/well) cells were cultured in six-well plates after treatment with compounds **9b** and **9e** at 0.5 and 1 μM concentrations for 48 h. After 48 h of treatment, cells were collected by trypsinization and washed with PBS followed by resuspending in

JC-1 (5 $\mu\text{g}/\text{mL}$) and incubated at 37 °C for 15 min. Cells were rinsed three times with medium and suspended in pre warmed medium. The cells were then subjected to flow cytometric analysis on a flow cytometer (Becton Dickinson) in the FL1, FL2 channel to detect mitochondrial potential [17].

3.1.22. ROS generation

The production of ROS (reactive oxygen species) was measured by flow cytometry using DCFDA (2',7'-dichlorofluoresceindiacetate) as previously described [18]. In this study MCF-7 cells were treated with compound **9b** and **9e** at 0.5 and 1 μM concentrations for 48 h. After treatment, cells were incubated with DCFDA (2 μM) at 37 °C for 30 min and then measured with the flow cytometer (FACS).

3.1.23. Annexin staining assay for apoptosis

MCF-7 (1×10^6) were seeded in six-well plates and allowed to grow overnight. The medium was then replaced with complete medium containing compounds **9b** and **9e** at 0.5 and 1 μM concentrations. After 48 h of drug treatment, cells from the supernatant and adherent monolayer cells were harvested by trypsinization, washed with PBS at 3000 rpm. Then the cells were stained with Annexin V-FITC and propidium iodide using the Annexin-V-FITC apoptosis detection kit (Sigma Aldrich). Flow cytometry was performed for this study as described earlier [19].

3.1.24. Activation of caspase 9

Caspase-9 assay was conducted for detection of apoptosis in breast cancer cell line (MCF-7). The commercially available apoptosis detection kit (Sigma Aldrich) was used. MCF-7 cells were treated with compounds **9b** and **9e** at 1 μM concentration for 48 h. After 48 h of treatment, cells were collected by centrifugation, washed once with PBS, and cell pellets were collected. Suspended the cell pellet in lysis buffer and incubated for 15 min. After incubation, cells were centrifuge at 20,000 rpm for 15 min and collected the supernatant. Supernatants were used for measuring caspase 9 activity using an ELISA-based assay, according to the manufacturer's instructions.

3.1.25. Protein extraction and western blot analysis

MCF-7 cells were treated with compounds **9b** and **9e** at 0.5 and 1 μM concentrations for 48 h. The cell lysates were obtained by lysing the cells in ice-cold radioimmunoprecipitation assay (RIPA) buffer (1 \times PBS, 1% NP-40 detergent, 0.5% sodium deoxycholate, and 0.1% SDS) containing 100 mg/mL phenylmethanesulfonyl fluoride (PMSF), 5 mg/mL aprotinin, 5 mg/mL leupeptin, 5 mg/mL pepstatin, and 100 mg/mL NaF. After centrifugation at 12000 rpm for 10 min, the protein in the supernatant was quantified by the Bradford method (BIO-RAD) by using a Multimode Varioskan instrument (Thermo Fischer Scientific Ltd.). Protein (50 μg per lane) was applied in 12% SDS polyacrylamide gel. After electrophoresis, the protein was transferred to a polyvinylidene difluoride (PVDF) membrane (Thermo Scientific Inc.). The membrane was blocked at room temperature for 2 h in Tris-buffered saline (TBS) with 0.1% Tween 20 (TBST) containing 5% blocking powder (Santa Cruz). The membrane was washed with TBST for 5 min, then primary antibody was added and the membrane was incubated for overnight. After incubation the membrane was incubated with the corresponding horseradish peroxidase labeled secondary antibody at room temperature for 1 h. Membranes were washed with TBST three times for 15 min, and the blots were visualized with chemiluminescence reagent. Images were captured by using the chemiluminescence (viber jourmat) [20].

Acknowledgment

This work was funded by CSIR, New Delhi under the XIIth Five year plan project 'Affordable Cancer Therapeutics-ACT' (CSC-0301). SA thanks CSIR-New Delhi and DY thanks UGC-New Delhi for providing fellowships.

Appendix A. Supplementary data

Supplementary data related to this article can be found at <http://dx.doi.org/10.1016/j.ejmech.2015.06.050>.

References

- [1] (a) B.M. Padhy, Y.K. Gupta, Drug repositioning: re-investigating existing drugs for new therapeutic indications, *J. Postgrad. Med.* 57 (2011) 153–160; (b) A.M. Virshup, J. Contreras-García, P. Wipf, W. Yang, D.N. Beratan, Stochastic voyages into uncharted chemical space produce a representative library of all possible drug-like compounds, *J. Am. Chem. Soc.* 135 (2013) 7296–7303.
- [2] J.P. Hughes, S. Rees, S.B. Kalindjian, K.L. Philpott, Principles of early drug discovery, *Brit. J. Pharmacol.* 162 (2011) 1239–1249.
- [3] (a) A. Jemal, F. Bray, M.M. Center, J. Ferlay, E. Ward, D. Forman, Global cancer statistics, *CA Cancer J. Clin.* 61 (2011) 69–90; (b) C.M. Barton, S.L. Staddon, C.M. Hughes, P.A. Hall, C. O'Sullivan, G. Kloppel, B. Theis, R.C.G. Russell, J. Neoptolemos, R.C.N. Williamson, D.P. Lane, N.R. Lemoine, Abnormalities of the p53 tumour suppressor gene in human pancreatic cancer, *Brit. J. Cancer* 64 (1991) 1076–1082.
- [4] S. Archana, R. Geesala, N.B. Rao, S. Satpati, G. Puroshottam, A. Panasa, A. Dixit, A. Das, A.K. Srivastava, Development of constrained tamoxifen mimics and their anti-proliferative properties against breast cancer cells, *Bioorg. Med. Chem. Lett.* 25 (2015) 680–684.
- [5] I. Meikle, J. Cummings, J.S. Macpherson, J.F. Smyth, Induction of apoptosis in human cancer cell lines by the novel anthracenylamino acid topoisomerase I inhibitor NU/ICRF 505, *Brit. J. Cancer* 74 (1996) 374–379.
- [6] K. Kuramochi, K. Fukudome, I. Kuriyama, T. Takeuchi, Y. Sato, S. Kamisuki, K. Tsubaki, F. Sugawara, H. Yoshida, Y. Mizushima, Synthesis and structure–activity relationships of dehydroaltenusin derivatives as selective DNA polymerase α inhibitors, *Bioorg. Med. Chem.* 17 (2009) 7227–7238.
- [7] G.T. Wondrak, Redox-directed cancer therapeutics: molecular mechanisms and opportunities, *Antioxid. Redox Signal* 11 (2009) 3013–3069.
- [8] J.S. Bair, R. Palchaudhuri, P.J. Hergenrother, Chemistry and biology of deoxyxyboquinone, a potent inducer of cancer cell death, *J. Am. Chem. Soc.* 132 (2010) 5469–5478.
- [9] D.C. Wallace, Mitochondria and cancer, *Nat. Rev. Cancer* 12 (2012) 685–698.
- [10] S. Fulda, L. Galluzzi, G. Kroemer, Targeting mitochondria for cancer therapy, *Nat. Rev. Drug Disc.* 9 (2010) 447–464.
- [11] (a) B. Antonsson, Mitochondria and the Bcl-2 family proteins in apoptosis signaling pathways, *Mol. Cell Biochem.* 256–257 (2004) 141–155; (b) T. Taguchi, Y. Kato, Y. Baba, G. Nishimura, Y. Tanigaki, C. Horiuchi, I. Mochimatsu, M. Tsukuda, Protein levels of p21, p27, cyclin E and Bax predict sensitivity to cisplatin and paclitaxel in head and neck squamous cell carcinomas, *Oncol. Rep.* 11 (2004) 421.
- [12] (a) P. Skehan, R. Storeng, D. Scudiero, A. Monks, J. McMahon, D. Vistica, J.T. Warren, H. Bokesch, S. Kenney, M.R. Boyd, New colorimetric cytotoxicity assay for anticancer-drug screening, *J. Natl. Cancer Inst.* 82 (1990) 1107–1112; (b) L.V. Rubinstein, R.H. Shoemaker, K.D. Paull, R.M. Simon, S. Tosini, P. Skehan, D.A. Scudiero, A. Monks, M.R. Boyd, Comparison of *in vitro* anticancer-drug screening data generated with a tetrazolium assay versus a protein assay against a diverse panel of human tumor cell lines, *J. Natl. Cancer Inst.* 82 (1990) 1113–1118.
- [13] (a) J. Massague, G1 cell-cycle control and cancer, *Nature* 432 (2004) 298–306; (b) M. Caputi, G. Russo, V. Esposito, A. Mancini, A. Giordano, Role of cell-cycle regulators in lung cancer, *J. Cell Physiol.* 205 (2005) 319–327.
- [14] Y. Luo, J. Hurwitz, J. Massague, Cell-cycle inhibition by independent CDK and PCNA binding domains in p21Cip1, *Nature* 375 (1995) 159.
- [15] V. Vichai, K. Kirtikara, Sulforhodamine B colorimetric assay for cytotoxicity screening, *Nat. Protoc.* 1 (2006) 1112.
- [16] M. Szumilak, M.A. Szulawska, K. Koprowska, M. Stasiak, W. Lewgowd, A. Stanczak, M. Czyz, Synthesis and *in vitro* biological evaluation of new polyamine conjugates as potential anticancer drugs, *Eur. J. Med. Chem.* 45 (2010) 5744–5751.
- [17] B. Chakravarti, M. Ranjani, J.A. Siddiqui, B. Hemant Kumar, S.M. Rajendran, Prem P. Yadav, K. Rituraj, *In vitro* anti-breast cancer activity of ethanolic extract of *Wrightia tomentosa*: role of pro-apoptotic effects of oleanolic acid and ursolic acid, *J. Ethnopharm.* 142 (2012) 72–79.
- [18] G. Ding, F. Liu, T. Yang, Y. Jiang, H. Fu, Y. Zhao, A novel kind of nitrogen heterocycle compound induces apoptosis of human chronic myelogenous leukemia K562 cells, *Bioorg. Med. Chem.* 14 (2006) 3766–3774.
- [19] L.J. Browne, C. Gude, H. Rodriguez, R.E. Steele, A. Bhatnager, Fadrozole hydrochloride: a potent, selective, nonsteroidal inhibitor of aromatase for the treatment of estrogen-dependent disease, *J. Med. Chem.* 34 (1991) 725–736.
- [20] G. Shafi, A. Munshi, T.N. Hasan, A.A. Alshatwi, A. Jyothy, D.K. Lei, Induction of apoptosis in HeLa cells by chloroform fraction of seed extracts of *Nigella sativa*, *Cancer Cell. Intern.* 9 (2009) 29.